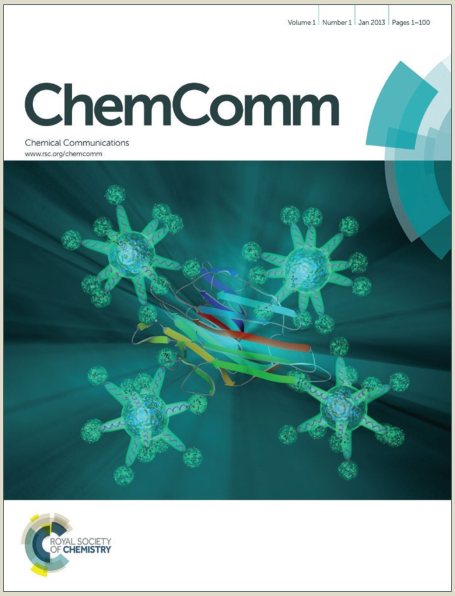
Volume 1 | Number 1 | Jan 2013 | Pages 1–100
ChemComm
Chemical Communications
www.rsc.org/chemcomm
ROYAL SOCIETY OF CHEMISTRY

Journal Name

COMMUNICATION

Controllable Synthesis of Hollow Mesoporous Silica Particles by a Facile One-Pot Sol-Gel Method

Received 00th January 20xx,
Accepted 00th January 20xx

DOI: 10.1039/x0xx00000x

www.rsc.org/

Jing-Chuan Song,[a] Fei-Fei Xue,[b] Zhong-Yuan Lu,[c] and Zhao-Yan Sun*[a]

A simple and facile one-pot sol-gel method is proposed for the fabrication of hollow mesoporous silica particles. Both the particle size and the shell thickness can be well controlled by moderately tuning some experimental parameters.

The synthesis of hollow mesoporous silica has received burgeoning attention in recent years due to their superior performance in some applications, such as catalysis,[1-4] biomedicine[5-10] and photonic band-gap materials.[11,12] To date, the templating methods are well-known strategies to synthesize hollow mesoporous silica particles, such as soft-templating method and hard-templating method. For soft-templating method, the hollow mesoporous particles are generally prepared by using the self-assembly of silicate with surfactants or gas bubbles templates.[13-17] But they are usually unstable, making it difficult to control the uniformity, dispersity and morphology. Although several examples have been reported so far for synthesizing uniform hollow mesoporous silica particles by using the soft-templating method, the control of the particle size and shell thickness is still a known drawback of these strategies.[18-21] Compared with the soft-templating method, the hard-templating method is more feasible, and the obtained hollow mesoporous silica particles in this way are more uniform. For the hard-templating method, the silica shells are firstly coated on the pre-prepared sacrificial particles and then the central hard cores are selectively removed by physical or chemical procedures, resulting in hollow mesoporous silica particles.[4,22-28] Nevertheless, the synthesis of parent particles (such as polystyrene particles and inorganic beads) are complicated and time-consuming. In addition, the morphology and the hollow core size of the resultant hollow mesoporous silica particles are limited to the pre-prepared parent particles. Moreover, self-templating method has also been used to prepare hollow mesoporous silica particles, but it usually needs some extremely corrosive etching agents or tedious multistep procedures, and the protective polymers and etching agents are hard wash away.[3, 29-32] Thus this method is also limited. Recently, Lu and coworkers developed a spontaneous self-transformation approach for the synthesis of silica hollow spheres with ordered mesopores.[33] Unfortunately, this technique results in lower yield (less than 50% when the size is below 550 nm) of hollow particles, time-consuming and the aggregation of particles is difficult to be avoided.

In recent years, analogues to the method of synthesizing silica particles has been successfully extended to synthesize resorcinol/formaldehyde spheres, which possesses the similar reaction mechanism of silicate.[34,35] Various resin-silica nanocomposite structures can be prepared when the silicate is introduced into the resol reaction systems.[36] In some cases, hollow silica can also be obtained after removing the resin in the composite nanoparticles. However, the controllability of particle size and shell thickness was inefficient, since the above-mentioned methods can only monotonously tune the size of particles and shell thickness, i. e., the shell thickness increases with increasing the particle size or decreases with decreasing the particle size. Moreover, the obtained particles were polydisperse in size. Due to the growing demand in different applications for hollow silica particles, it is highly desirable to develop a simple, effective approach for preparing hollow silica particles with different size/shell ratio while keeping high success rate and high reproducibility.

Recently, it was found that the 3-aminophenol/formaldehyde resin system possessed some advantages compared with resorcinol/formaldehyde system.[37,38] The hydrolysis rate of 3-aminophenol/formaldehyde is faster and the resultant particles display perfect monodispersity in size. Herein inspired by these advantages of 3-aminophenol/formaldehyde reaction system and using the similarities of hydrolysis reaction mechanism between phenolic resin and silicate, we report the preparation of monodisperse hollow mesoporous silica particles with controllable particle size and shell thickness by a facile one-pot sol-gel method. The approach is very simple and effective. More importantly, the

---

[a] *State Key Laboratory of Polymer Physics and Chemistry Changchun Institute of Applied Chemistry, Chinese Academy of Sciences, Changchun 130022 China.*
Fax: +86 431 85262969, E-mail: zysun@ciac.ac.cn.
[b] *Department School of Materials Science and Engineering, Tianjin University, Tianjin 300072, China.*
[c] *Institute of Theoretical Chemistry, State Key Laboratory of Supramolecular Structure and Materials, Jilin University, Changchun, China.*

†Electronic Supplementary Information (ESI) available: Experimental section, Table S1 and Fig. S1–S9. See DOI: 10.1039/x0xx00000x

obtained particle size and shell thickness can be tuned bi-directionally by changing the concentration of TEOS and 3-aminophenol, and the volume ratio of ethanol/water, i. e., the shell thickness increases or decreases with the increase of particle size. The obtained mesoporous hollow silica particles possess high surface area and accessible mesopores. Scheme 1 illustrates the detailed formation process of hollow mesoporous silica. In a mixture of ethanol, water, TEOS, 3-aminophenol, formaldehyde, hexadecyl trimethylammonium chloride (CTAC) and ammonia aqueous solution, the sol-gel of 3-aminophenol/formaldehyde takes place firstly under the catalysis of ammonia due to its faster hydrolysis rate than TEOS, and the resultant resin particles act as sacrificial particles in the following silica coating process. Subsequently, TEOS derived silica oligomers assemble with the CTAC and diffuse to the pre-formed resin particles, resulting uniform silica shells with mesostructures. After calcining off the phenolic resin and CTAC, highly monodisperse hollow mesoporous silica spheres are obtained.

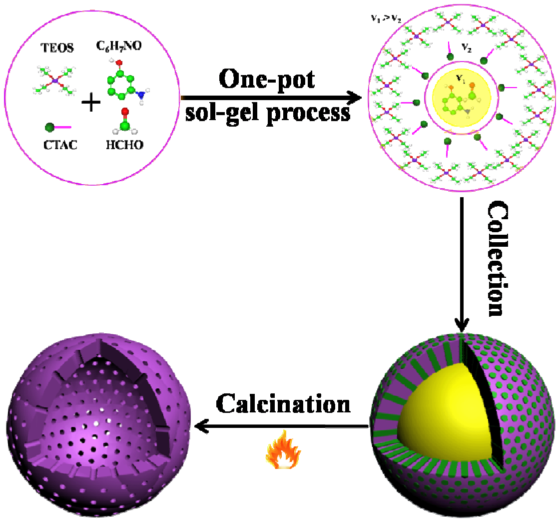

Scheme 1 Preparation strategy of the hollow mesoporous silica spheres by using a facile one-pot sol-gel process. V_1 refers to the hydrohydrolysis rate of 3-aminophenol/formaldehyde and V_2 corresponds to the hydrolysis rate of TEOS.

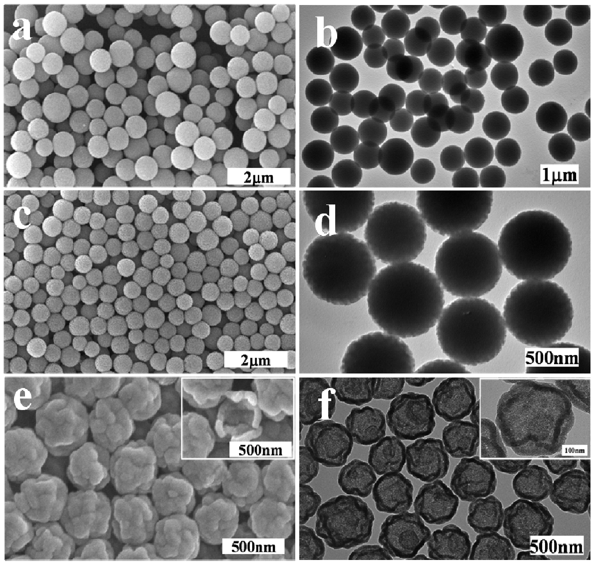

Fig. 1 a) FE-SEM image and b) TEM image of as-made resin/silica nanocomposite particles, c) and d) are FE-SEM image and TEM image of resin particles after etching silica, respectively, e) FE-SEM image of hollow silica particles and f) the corresponding TEM image of hollow silica particles. The inset in e shows a crushed particle and inset in f is a high-magnification image of a hollow silica particle.

Fig. 1a and b show the field emission scanning electron microscopy (FE-SEM) image and transmission electron microscopy (TEM) image of a typical resin/silica composite nanoparticles synthesized at 0.72 ml of TEOS, 0.2 g of 3-aminophenol, 0.28 ml of formaldehyde, CTAC solution (0.83 ml, 25 wt% in water), 8 ml of ethanol, 0.1 ml of NH_4OH and 19 ml of water, respectively. The detailed synthesis processes are given in Table S1 (ESI†). Obviously, the as-made composite nanoparticles have uniform spherical structure. After etching silica with hydrofluoric acid (HF, 15wt%), the resin particles were obtained, as seen in the FE-SEM image (Fig. 1c) and TEM image (Fig. 1d). The images reveal that the resulted particles retain solid spheres and present some pits on the surface. The results confirm the proposed mechanism in the above-mentioned scheme that resin particles form firstly in the sol-gel process and then the silica shells deposit on the preformed resin particles. Fig. 1 e and f show FE-SEM and TEM images of the obtained silica particles after calcinating resin/silica nanocomposite particles in the air. Interestingly, as seen in Fig. 1e, the obtained particles display crumpled spherical morphology. Although the hydrolysis rate of 3-aminophenol/formaldehyde is much faster than that of TEOS, it is inevitable that some resins will also exist in the outside part of the particles together with the silica. After calcining, both of the inner part and the outside part of the resins are removed, resulting in the collapse of the silica part and the crumpled spherical morphology of the hollow silica particles. The hollow mesoporous silica particles display well-dispersed with a uniform size of 440 nm. The detailed size distribution obtained from more than 200 particles in the FE-SEM images is shown in Fig. S1b (ESI†). The FE-SEM image of a crushed silica particle clearly reveals the hollow structure (inset in Fig. 1e). The corresponding TEM image further confirms the hollow structure of the resulting silica particles (Fig. 1f), in which the shells appear dark. The shell thickness of the hollow silica particles measured from the TEM images is around 60 nm (Fig. S2, ESI†). The high-magnification image of a hollow silica particle reveals that the shell possesses accessible mesopores throughout the shell (inset in Fig. 1f). To further confirm the accessibility of mesopores more intuitionisticly, we did extra saline-loaded experiment (ESI†). The TEM image demonstrates that the NaCl-microcrystals are loaded into the hollow mesoporous silica through the mesopores successfully (Fig. S3, ESI†). The rapid loading rate of NaCl-microcrystals is attributed to the accessibility of the mesopores. Nitrogen sorption of the obtained mesoporous silica shows a type IV isotherm, indicating the presence of mesopores. It possesses a high Brunauer-Emmett-Teller (BET) surface area of 644 m^2/g and the total pore volume is as high

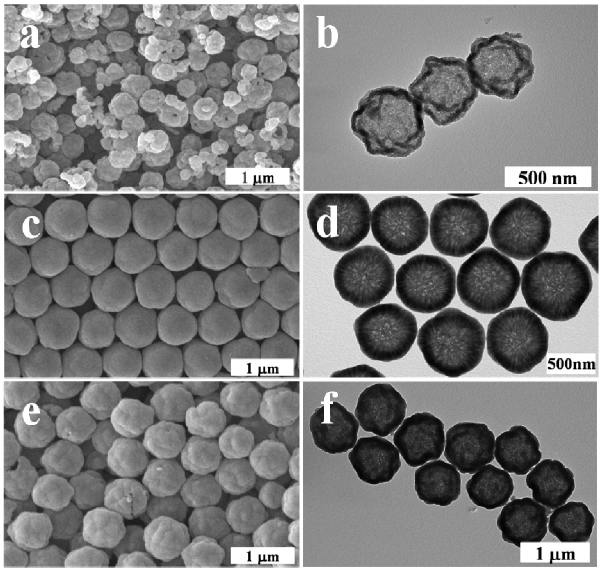

Fig. 2 FE-SEM images (a, c and e) and TEM images (b, d and f) of hollow silica particles prepared at different concentration of TEOS. a) and b) 0.36 ml, c) and d) 1.08 ml, e) and f) 1.44ml.

as 0.82 cm^3/g (Fig. S11b, ESI†).

The size and shell thickness can be controlled by tuning the concentration of precursor (TEOS or 3-aminophenol). As shown in Fig. 2, the particle size and shell thickness increase with increasing the TEOS concentration. The increase of TEOS concentration makes more silica deposit on the resin particles, leading to larger hollow mesoporous silica and thicker shells. As the volume of TEOS increases from 0.36 to 1.08 and 1.44 ml, the size of hollow mesoporous silica increases from 420 to 655 and 690 nm and the shell thickness increases from 36 to 103 and 112 nm, respectively. The detailed size distribution is shown in Fig. S1 (ESI†). It is worth mentioning that there were no free solid silica spheres found when increasing the concentration of TEOS (the amount of TEOS is in the range of 0.36 to 1.44 ml, and the amount of 3-aminophenol is 0.2g). Therefore, the secondary nucleation could be avoided in the studied amount of TEOS and 3-aminophenol. If the amount of TEOS is further increased to a very high level, the secondary nucleation will occur in the reactant. Then one can use centrifugation to separate the solid silica spheres from the desired core-shell product since the size of solid spheres is often smaller than the composite particles.

From aforementioned discussion we know that the content of TEOS can monotonously tune the size of particles and shell thickness. More interestingly, the concentration of 3-aminophenol can tune them in opposite direction, i.e., the shell thickness increases with decreasing particles size (The detailed synthesis conditions are given in Table S1, see sample 2, 5 and 6, ESI†). With the concentration of 3-aminophenol reducing from 0.2 to 0.1 g, the hollow mesoporous silica size decreases from 440 to 270 nm and the shell thickness increases to 95 nm (Fig. S5, ESI†). With the decrease of 3-aminophenol concentration, polymerization rate reduces and smaller resin particles are produced as well as relatively thicker silica shells form. When the concentration of 3-aminophenol decreased to 0.05 g, no hollow silica particles were observed. The corresponding FE-SEM images and TEM images are shown in Fig. S6 (ESI†). The as-made silica/resin produces present some smaller particles and blocky products (Fig. S6a and d, ESI†). After etching with HF, only blocky products are kept, which demonstrates the obtained particles are silica spheres (Fig. S6b and e, ESI†). This can also be confirmed from the FE-SEM, TEM images and infrared spectra of calcinating samples (Fig. S6c and f, Fig S7 ESI†). There is no hollow structure present and the characteristic peaks of aliphatics at 2850-2950 cm^{-1} in the infrared spectra of the calcinating samples disappear, confirming the complete removal of resin[23] and the surviving solid spheres are solid silica particles. Such structure is formed because the concentration of 3-aminophenol is so low that the polymerization speed of TEOS becomes larger than that of resin, resulting no resin core forms in the silica particles. The corresponding BET surface area and total pore volume are 1146 m^2/g, 1156 m^2/g and 1.11 cm^3/g, 1.70 cm^3/g, respectively (Fig. S11, ESI†).

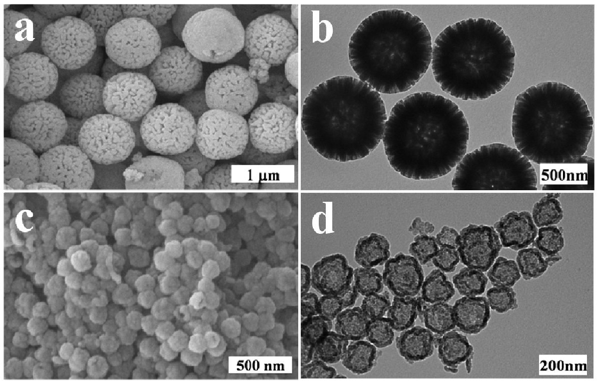

Fig. 3 FE-SEM images (a and c) and TEM images (b and d) of hollow silica particles prepared at different volume of ethanol. a) and b) 10 ml, c) and d) 6 ml.

Also, the structures of hollow mesoporous silica correlate with the volume ratio of ethanol/water (sample 2, 7, 8 and 9 ESI†). The particle size and the shell thickness increase with increasing the volume of ethanol (Fig. S2 and S10, ESI†). When the volume ratio of ethanol/water is 10/19, the hollow silica size is ~890 nm and the shell thickness is ~197 nm (Fig. 3a and b). As shown in the FE-SEM image of resulted hollow silica particles, some large pores present which may come from calcinating the resin particles. The increase of ethanol can accelerate the solution of TEOS in the mixing solvent, which leads to the increase of the formation speed of silica shell. With the volume ratio of ethanol/water decreasing to 6/19, smaller hollow silica particles (170 nm) and thinner shells (22 nm) are obtained (Fig. 3c and d). Further decreasing the volume of ethanol (4 ml), sub-100 nm hollow silica particles are produced (Fig. S9, ESI†)). The resulting particles also exhibit high surface area and large pore volume (Fig. S11, ESI†).

In summary, we have demonstrated a new strategy to synthesizing hollow mesoporous silica particles. The approach is very simple and facile. The obtained hollow mesoporous silica particles present a uniform spherical structure and display highly monodispersity in size. The size and shell thickness can be effectively tuned in bi-directionally. The size and shell thickness of particles can be easily controlled in the range of 85-890 nm and 14-197 nm, respectively, by varying the concentration of TEOS or 3-aminophenol and the volume ratio of ethanol/water. Moreover, the hollow silica particles possess high surface area and pore volume. The mesopores are accessible in the shells. The conception reported in this study may provide a new avenue for the fabrication of more nanostructured silica particles.

This work is subsidized by the National Basic Research Program of China (973 Program, 2012CB821500). The authors also appreciate the financial support from the National Science Foundation of China (21222407, 21474111).

Notes and references

1 Q. Zhang, X. Shu, J. M. Lucas, F. D. Toste, G. A. Somorjai and A. P. Alivisatos, *Nano Lett.*, 2014, **14**, 379.
2 F. Chang, Y. Chen and C. Mou, *Small*, 2014, **10**, 4785.
3 X. Fang, Z. Liu, M.-F. Hsieh, M. Chen, P. Liu, C. Chen, and N. Zheng, *ACS Nano*, 2012, **6**, 4434.
4 Z. Chen, Z. Cui, F. Niu, L. Jiang and W. Song, *Chem. Commun.*, 2010, **46**, 6524.
5 Z. Luo, Y. Hu, K. Cai, X. Ding, Q. Zhang, M. Li, X. Ma, B. Zhang, Y. Zeng, P. Li, J. Li, J. Liu and Y. Zhao, *Biomaterials*, 2014, **35**, 7951.
6 P. Yang, S. Gai and J. Lin, *Chem. Soc. Rev.*, 2012, **41**, 3679.
7 Y. Chen, H. Chen, Y. Sun, Y. Zheng, D. Zeng, F. Li, S. Zhang, X. Wang, K. Zhang, M. Ma, Q. He, L. Zhang and J. Shi, *Angew. Chem.*, 2011, **123**, 12713.
8 Y. Chen, H. Chen, L. Guo, Q. He, F. Chen, J. Zhou, J. Feng and J. Shi, *ACS Nano*, 2010, **4**, 529.
9 Y. Zhu, T. Ikoma, N. Hanagata and S. Kaskel, *Small*, 2010, **6**, 471.
10 Y. Zhu, J. Shi, W. Shen, X. Dong, J. Feng, M. Ruan and Y. Li, Angew. Chem., *2005*, **117**, 5213.
11 L. A. Fielding, O. O. Mykhaylyk, A. Schmid, D. Pontoni, S. P. Armes and P. W. Fowler, *Chem. Mater*., 2014, **26**, 1270.
12 T. Deng and F. Marlow, *Chem. Mater*., 2012, **24**, 536.
13 J. Wang, F. Li, H. Zhou, P. Sun, D. Ding and T. Chen, *Chem. Mater*., 2009, **21**, 612.
14 R. K. Rana, Y. Mastai and A. Gedanken, *Adv. Mater*., 2002, **14**, 1414.
15 H. Djojoputro, X. F. Zhou, S. Z. Qiao, L. Z. Wang, C. Z. Yu, and G. Q. Lu, *J. Am. Chem. Soc.,* 2006, **128**, 6320.
16 J. Li, J. Liu, D. Wang, R. Guo, X. Li and W. Qi, *Langmuir,* 2010, **26**, 12267.
17 S. Schacht, Q. Huo, I. G. Voigt-Martin, G. D. Stucky and F. Schüth, *Science*, 1996, **273**, 768.
18 Z. Feng, Y. Li, D. Niu, L. Li, W. Zhao, H. Chen, L. Li, J. Gao, M. Ruan and J. Shi, *Chem. Commun*., 2008, 2629.
19 Y. Zhao, J. Zhang, W. Li, C. Zhang and B. Han, *Chem. Commun*., 2009, 2365.
20 D. Wang and H. Zeng, *Chem. Mater*., 2011, **23**, 4886.
21 M. Wang, Q. Zeng, B. Zhao and D. He, *J. Mater. Chem. A*, 2013, **1**, 11465.
22 B. Tan and S. E. Rankin, *Langmuir*, 2005, **21**, 8180.
23 H. Blas, M. Save, P. Pasetto, C. Boissiere, C. Sanchez and B. Charleux, *Langmuir*, 2008, **24**, 13132.
24 Y. Yamada, M. Mizutani, T. Nakamura and K. Yano, *Chem. Mater*., 2010, **22**, 1695.
25 Y. Zhao, L. Lin, Y. Lu, S. Chen, L. Dong and S. Yu, *Adv. Mater.*, 2010, **22**, 5255.
26 T. Wang, F. Chai, Q. Fu, L. Zhang, H. Liu, L. Li, Y. Liao, Z. Su, C. Wang, B. Duan and D. Ren, *J. Mater. Chem.*, 2011, **21**, 5299.
27 S. I.R. Castillo, S. Ouhajji, S. Fokker, B. H. Erné, C. T.W.M. Schneijdenberg, D. M.E. Thies-Weesie and A. P. Philipse, *Microporous Mesoporous Mater.*, 2014, **195**, 75.
28 M. Hembury, C. Chiappini, S. Bertazzo, T. L. Kalber, G. L. Drisko, O. Ogunlade, S. Walker-Samuel, K. S. Krishna, C. Jumeaux, P. Beard, C. S. S. R. Kumar, A. E. Porter, M. F. Lythgoe, C. Boissière, C. Sanchez and M. M. Stevens, *Proc. Natl. Acad. Sci. USA.*, 2015, **112**, 1959.
29 X. Fang, C. Chen, Z. Liu, P. Liu and N. Zheng, *Nanoscale*, 2011, **3**, 1632.
30 Y. J. Wong, L. Zhu, W. S. Teo, Y. W. Tan, Y. Yang, C. Wang and H. Chen, *J. Am. Chem. Soc*., 2011, **133**, 11422.
31 Q. Zhang, T. Zhang, J. Ge and Y. Yin, *Nano Lett*., 2008, **8**, 2867.
32 T. Zhang, J. Ge, Y. Hu, Q. Zhang, S. Aloni and Y. Yin, *Angew. Chem. Int. Ed.*, 2008, **47**, 5806.
33 Z. Teng, X. Su, Y. Zheng， J. Sun, G. Chen, C. Tian, J. Wang, H. Li, Y. Zhao and G. Lu, *Chem. Mater*., 2013, **25**, 98.
34 J. Liu, S. Z. Qiao, H. Liu, J. Chen, A. Orpe, D. Zhao and G. Q. Lu, *Angew. Chem. Int. Ed*., 2011, **50**, 5947.
35 J. Liu, T. Yang, D. Wang, G. Q. Lu, D. Zhao and S. Z. Qiao, *Nat. Commun.*, 2013, **4**, 2798.
36 Z. Qiao, B. Guo, A. J. Binder, J. Chen, G. M. Veith and S. Dai, *Nano Lett*., 2013, **13**, 207.
37 J. C. Song, Z. Y. Lu and Z. Y. Sun, *J. Colloid Interface Sci.*, 2014, **431**, 132.
38 J. Zhao, W. Niu, L. Zhang, H. Cai, M. Han, Y. Yuan, S. Majeed, S. Anjum and G. Xu, *Macromolecules*, 2013, **46**, 140.